Intent Pattern Recognition of Lower-limb Motion Based on Mechanical Sensors

Zuojun Liu, Wei Lin, Yanli Geng, and Peng Yang

***Abstract*—Based on the regularity nature of lower-limb motion, an intent pattern recognition approach for above-knee prosthesis is proposed in this paper. To remedy the defects of recognizer based on electromyogram (EMG), we develop a pure mechanical sensor architecture for intent pattern recognition of lower-limb motion. The sensor system is composed of an accelerometer, a gyroscope mounted on the prosthetic socket, and two pressure sensors mounted under the sole. To compensate the delay in the control of prosthesis, the signals in the stance phase are used to predict the terrain and speed in the swing phase. Specifically, the intent pattern recognizer utilizes intraclass correlation coefficient (ICC) according to the Cartesian product of walking speed and terrain. Moreover, the sensor data are fused via Dempster-Shafer's theory. And hidden Markov model (HMM) is used to recognize the realtime motion state with the reference of the prior step. The proposed method can infer the prosthesis user's intent of walking on different terrain, which includes level ground, stair ascent, stair descent, up and down ramp. The experiments demonstrate that the intent pattern recognizer is capable of identifying five typical terrain-modes with the rate of 95.8%. The outcome of this investigation is expected to substantially improve the control performance of powered above-knee prosthesis.**

***Index Terms*—Above-knee prosthesis, hidden Markov model (HMM), intra-class correlation coefficient (ICC), intent pattern recognition, sensor fusion.**

I. Introduction

THE major function of prosthetic legs is to restore the locomotion of amputees. The focus of the above-knee prostheses research is on the motion intent recognition and the control of the artificial knee joint [1], [2]. Some recent designs of above-knee prostheses have offered amputee patients improved safety, stability and the coordination with contralateral healthy limb, as well as the decrease in energy consumption. In addition, new developments in powered prosthesis design have further improved the function of prosthesis. These prosthetic legs can assist amputees with versatile activities beyond level ground walking. However, without knowing the amputees movement intent, which includes the terrain, speed and gait phase, the prostheses cannot select the correct control mode to adjust the joint impedance, or to drive powered joint motion in a proper manner [3].

Motion intent recognition based on electromyogram (EMG) has been widely reported in the literature. The authors of [1] introduced a phase-dependent surface EMG analysis method for the identification of locomotion modes. In [4], support vector machine (SVM) and linear-discriminant-analysis (LDA) were employed to analyze the EMG signals of residual thigh muscles. In addition, there are also other EMG signals analyzing approaches for motion intent recognition, such as artificial neural network, K-nearest neighbor (KNN) and multiple-binary classifier (MBC), to just name a few. Reference [5] proposed neural-machine interface (NMI) control structure for the above-knee prosthesis based on EMG. Furthermore, [6] developed a brain-machine interface (BMI) prosthesis based on electroencephalogram (EEG).

There are also other sensor signals that are involved and fused with EMG signals for intent pattern recognition. The EMG signals and ground reaction forces/moments (GRF) measured from the prosthetic pylon were utilized in [7] and [8] for locomotion-mode identification. The study of [9] illustrated that a combination of EMG and non-contact capacitive sensor (C-Sens) can improve the motion classification accuracy, in which the C-Sens detects changes in physical distance between the residual limb and the prosthesis.

Pattern recognition based on EMG or myoelectric control of above-knee prostheses has shown a great potential in research. However, myoelectric control systems for above-knee prosthesis perform poorly in clinical trials, due to the presence of electrode shift including the effects of socket loading, limb orientation, variations in muscle contraction effort, changes in electrode position during donning/doffing and daily use [10]. Moreover, it also faces other challenging issues such as different residual muscles conditions of amputees, the sweat, the vibrating interference caused by walking, the muscles and nerve atrophy, etc. The most serious drawback of myoelectric control is the lack of generality. To be more specific, a myoelectric control system for above-knee prostheses does not work well for different amputees [11]. The rehabilitation technicians have to regulate it laboriously and the amputees have to suffer a tedious training process. As a result, myoelectric

Manuscript received May 29, 2016; accepted January 16, 2017. This work was supported in part by the National Nature Science Fundation (61174009, 61203323), Youth Foundation of Hebei Province (F2016202327), and the Colleges and Universities in Hebei Province Science and Technology Research Project (ZC2016020). Wei Lin's work was supported in part by Key Project of NSFC (61533009), 111 Project (B08015), and Research Project (JCYJ20150403161923519). Recommended by Associate Editor Jian Yang. *(Corresponding author: Zuojun Liu.)*

Citation: Z. J. Liu, W. Lin, Y. L. Geng, and P. Yang, "Intent pattern recognition of lower-limb motion based on mechanical sensors," *IEEE/CAA J. of Autom. Sinica*, vol. 4, no. 4, pp. 651−660, Oct. 2017.

Z. J. Liu is with the School of Control Science and Engineering, Hebei University of Technology, Tianjin 300130, China, and also with the Engineering Research Center of Intelligent Rehabilitation, Ministry of Education, Tianjin 300130, China (e-mail: liuzuojun@hebut.edu.cn).

W. Lin is with the Department of Electrical Engineering and Computer Science, Case Western Reserve University, Cleveland, OH 44106, USA (e-mail: linwei@case.edu).

Y. L. Geng and P. Yang are with Hebei University of Technology, Tianjin 300130, China (e-mail: gengyanli318813@163.com; yphebu@aliyun.com).

Color versions of one or more of the figures in this paper are available online at http://ieeexplore.ieee.org.

Digital Object Identifier 10.1109/JAS.2017.7510619

control causes unacceptable cost and inconvenience, especially for the amputees in developing countries [12].

Pure mechanical sensor systems have also been proposed for limb intent recognition.

The paper [2] presented an activity-mode intent recognition framework based on a sensor package for measuring the socket interface moment, ground reaction force, and joint positions and torques, respectively. Separate Gaussian mixture models (GMM) were used for classifying the state of standing, sitting, and walking, but the activities associated with stairs were not involved.

In [13], a sensor system composed of accelerometer MMA7361L and gyroscopes ENC-03 is mounted on prosthetic socket. The KNN algorithm was used to identify amputees walking speed. Based on a portable laser distance sensor and an inertial measurement unit (IMU), a wearable terrain detection unit was employed to detect the terrain change in front of the prosthesis user [14]. In [15], thigh angle, shank angle, knee joint angle and plantar pressure signals were used for motion feature extraction via a BP neural network. In [16], the ground ramp was estimated via a three-axis accelerometer ADXL330 integrated into the prosthetic foot, wherein one of the measurement axes is aligned with the vertical when the foot is on level ground.

Wang *et al.* [17] proposed a method to identify different terrains based on the GRF sensors, but the motion information during swing phase could not be used. Chen *et al.* [18] identified different locomotion modes using wearable capacitive sensors. The inconvenience of this method was that the capacitive sensors had to be attached to the skin directly, which might aggravate the acceptance by amputees. Yuan *et al.* [19] presented a fuzzy-logic-based method, in which two force sensitive resistors (FSR), two gyroscopes, two accelerometers and a timer are utilized to identify different terrains and transitions. Young *et al.* [20] introduced a 13 IMU and motor current sensors system, including positions and velocities for both the knee and ankle's, axial loads. A linear discriminant analysis (LDA) classifier was used to classify locomotion mode. The shortcomings of methods in [19] and [18] were that too many sensors and heavy computations were needed. In addition, Li *et al.* [21] used the IMU to identify level ground, stair and ramp ascent/descent with a threshold method. The disadvantage of this method was that the identification had a delay of one step. In addition, there are also other motion intent recognition approaches based on mechanical sensors for below-knee amputee, old people, Parkinson patients, which are also beneficial for this research.

As summarized in [19], a good terrain identification method should meet the following requirements, which are high accuracy, minimal sensors, short delay, and low computation load. This is exactly what we propose in this paper. A mechanical sensor system includes an accelerometer, a gyroscope mounted on the prosthetic socket, and two pressure sensors mounted under the sole. To compensate the inherent delay in the control joint mechanism, only the signals in stance are used to predict the terrain and speed in the swing phase. The sensor signals are extracted by intraclass correlation coefficient (ICC) approach, sensor fusion and a hidden Markov model (HMM) algorithm. Such a method can infer the terrain mode, which includes level ground, stair ascent, stair descent, up ramp or down ramp, as well as the speed and gait phase. Experiments are carried out with three able-bodied and two amputee subjects to verify the effectiveness of the proposed method. The contribution of this paper is to provide a different and effective mechanical sensor system with its algorithm for the intent pattern recognition. The authors hope it might provide beneficial reference for the researchers in the same field.

The rest of this paper is organized as follows. Section II introduces the mechanical sensor system. Section III describes the intent pattern recognition method in detail, including the experimental protocol and algorithm process. Results and discussion are presented in Section IV. The conclusions are drawn in Section V.

II. Mechanical Sensor System and Experiment

When an amputee walks in different terrains, the acceleration and angle of residue limb are apparently different, so are the pressure of sole. Conversely, the signals of acceleration, angle of residue limb and the pressure of sole can reflect various motion intents. we propose in this section a mechanical sensor system for intent pattern recognition of lower-limb motion. Our sensor system contains an accelerometer, a gyroscope mounted on the prosthetic socket, and two pressure sensors mounted under the sole.

As shown in Fig. 1, the 4 sensors are attached on the same position on the prosthesis side of amputees or on the leg of abled-bodied men in this design, and no sensors are attached to the body or the healthy-side leg, in case of interfering with the amputee's motions. Additionally, the sensors are easily embedded into the prosthesis to improve convenience.

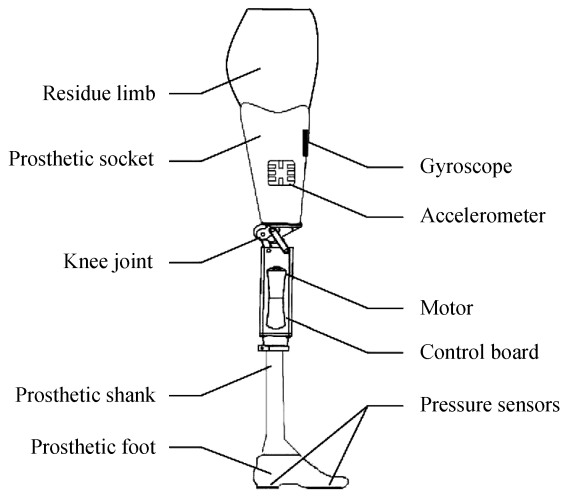

Fig. 1. Sensor system for intent pattern recognition.

A. Accelerometer

A MMA7361L type accelerometer is mounted at the side of the prosthetic socket, as shown in Fig. 1 and Fig. 2(a). To eliminate the spikes or glitches in the signals, a wavelet threshold denoising approach is used. As Sym6 wavelet has good symmetry and quadrature property, it shows good denoisng effect [22]. According to the character of prosthesis motion,

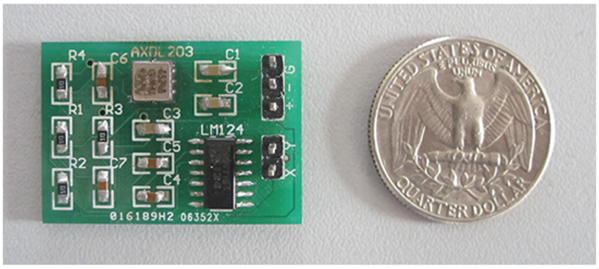

(a) Size of accelerometer

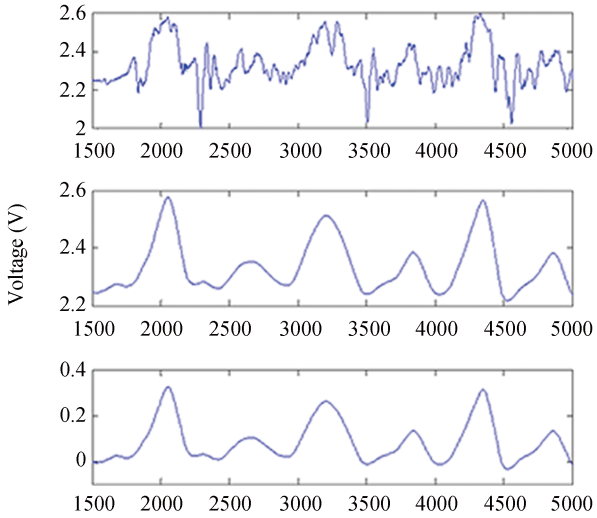

(b) Signals of accelerometer

Fig. 2. Accelerometer.

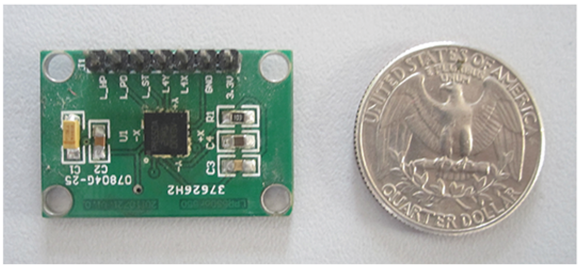

(a) Size of gyroscope

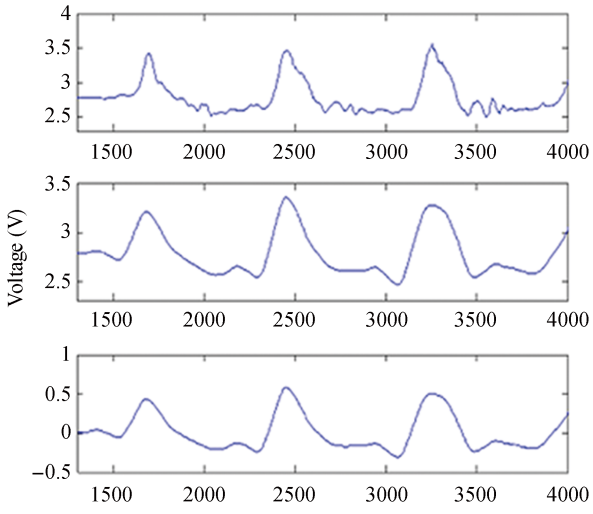

(b) Signals of gyroscope

Fig. 3. Gyroscope.

the accelerating signals of prosthesis are decomposed by 7-level wavelet and then processed via a low pass filter. The signals below 5 Hz are kept for signal reconstruction. As shown in Fig. 2(b), the top one is the original signal waveform. The middle one is the signal under wavelet threshold denoising. The bottom one is the signal after the digital zeroing and calibration. Such a pre-processing of the signals makes the analysis of prosthesis motion in Section III easier and more accurate.

B. Gyroscope

A NEC-03 type gyroscope is mounted at the front of the prosthetic socket, as shown in Fig. 1 and Fig. 3(a). A similar preprocessing of angular signals from gyroscope is also carried out. As illustrated in Fig. 3(b), the top one is the original signal waveform. The middle one is the signal under wavelet threshold denoising. The bottom one is the signal after the digital zeroing and calibration.

C. Pressure Sensors

Two pressure switches are mounted under the sole of the prosthetic foot, one under the ball flat and another under the heel, as shown in Fig. 1 and Fig. 4(a). The time sequence of square waveform signals from the pressure sensors divides a gait cycle into four phases. Firstly, the gait phase is defined as the early stance phase with the detection of heel strike. Secondly, the gait phase switches to the middle stance phase with the detection of ball flat contact. Thirdly, the gait phase switches to the late stance phase when heel is off the ground. Finally, the gait phase is in the swing phase when foot is off the ground. A similar idea could also be found in [19]. Take Fig. 4(b) as an example, the top one is the heel pressure signal. The middle one is the ball flat pressure signal. The bottom one is the four phases of a gait cycle. As pointed out in [14], [15], the pressure switches could also provide trigger for the cycle control of prosthesis.

D. Experiment Protocol

Three average height (1.68−1.75 m) and weight (65−76 kg) able-bodied men, aged 23−35, and two transfemoral (TF) amputees, aged 34 and 37, respectively, are recruited in our study. The TF amputees wore their own prosthesis (one is Otto Bock, and the other is Jingbo made in China. The sensor was reinforced on the prosthesis socket by elastic suspension belts. All the subjects received instructions and practised the tasks several times prior to measurement. Five terrain modes were investigated: level ground, stair ascent, stair descent, up and down ramp. Subjects were instructed to walk at slow, medium and fast speeds respectively. A 6-stair staircase was used for stair ascent/descent tests. The staircase was 15 cm high, 90 cm

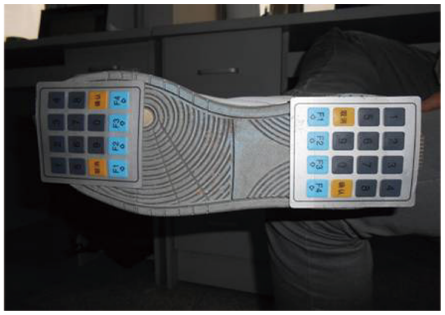

(a) Size of pressure sensors

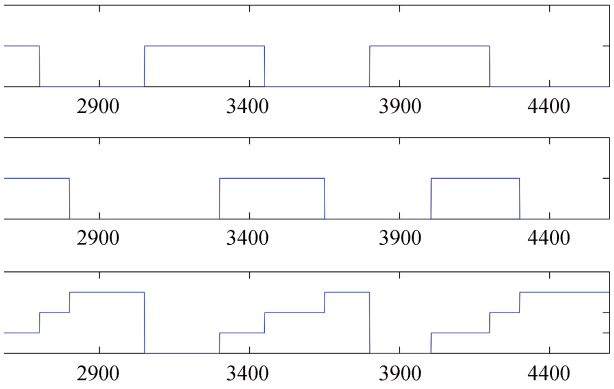

(b) Signals of pressure sensors

Fig. 4. Pressure sensors.

wide, and 30 cm deep. A 3.5 m long 15° ramp was used for up/down ramp test. The experiment platform is shown in Fig. 5(a). Figs. 5(b) and (c) to exhibit the experiment process.

In each trial, subjects performed one type of task. Each terrain mode was repeated for 4 turns, and each turn includes 6−8 steps. Except those abnormal ones, at least 20 complete stride of each terrain were recorded. Rest periods were arranged between trials to avoid fatigue.

III. Intent Pattern Recognition

The pre-recognition of terrain and the gait speed is the key for intent pattern recognition of lower-limb motion. In this section, we address this important issue by using the signals in stance phase to predict the terrain and speed in the swing phase, which turns out to be very effective in remedying the delay in the control of prosthesis. A detailed procedure is described and discussed in the next three subsections.

A. Intraclass Correlation Coefficient of Motion Signals

1) Cartesian Product: Walking on different terrains with different speeds, the accelerometer and gyroscope exhibit different features in the waveforms. By comparing the real-time waveforms with the standard waveform samples, the intent pattern might be recognized. The standard waveform samples are organized via the so-called Cartesian product. First, the terrains are divided into five typical categories including the level ground, stair ascent, stair descent, up ramp and down ramp, denoted by N. Then, a fuzzy speed set M is defined

(a) Multi-terrain platform

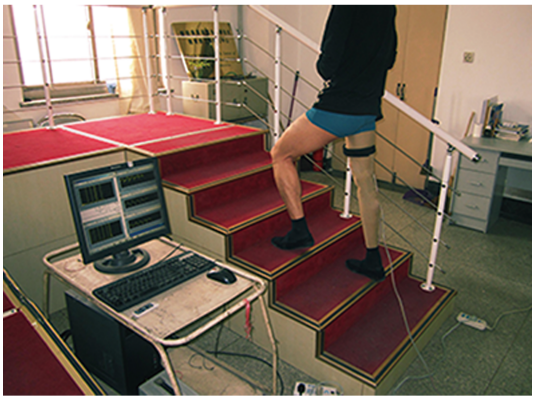

(b) Experiment of stair ascent

(c) Experiment of up ramp

Fig. 5. Experiments.

by taking into account of different amputee's walking speeds, which include fast speed of 3 km/h or higher, medium speed ranging from 2 km/h to 3 km/h, and slow speed of 2 km/h or lower. Last, a Cartesian product is defined as $N \times M$ [22]. As a such, all the typical motion patterns can be characterized by the set {(level ground, fast), ..., (stair ascent, medium speed), ..., (down ramp, slow)}, fifteen samples in all. The level of similarity can be measured by the intraclass correlation coefficient (ICC) method which will be introduced in the next paragraph. Take the samples at the medium speed as an example, the waveforms from the top to the bottom in Fig. 5 are the real time signals, and the standard signals of stair ascent, stair descent, up ramp, down ramp, and level ground,

respectively.

2) Intraclass Correlation Coefficient: The intraclass correlation coefficient (ICC) is a widely adopted method that has been used to measure the level of similarity between two signals.It is defined as the quotient of the covariance over standard deviation of two variables. The ICC approach has been used to diagnose movement symmetry in early Parkinsons disease [24]. Reference [25] used the ICC to evaluate a hip orthosis for paraplegia patients. In this paper, we choose the ICC approach to provide information about the terrain pattern similarity between outcomes from the accelerometer and gyroscope for the following consideration. When an amputee walks on the same terrain, the sensor signals exhibit a similar waveform. The ICC of the waveforms is high. Setting a signal template of walking patterns, one can calculate the ICC between the samples in the template and the real time walking signal. Furthermore, the signal templates are only effective for the similar height. If the height or walking style is different, the signal template is different too. So do the templates of able-body and amputees.

Specifically, the ICC is computed as follows. First, the sensor data are recorded from the beginning of stance phase. According to the statistics, the stance phase of amputees is usually from 0.8 to 1.0 second. As the sampling frequency is 500 Hz, so the sampling points are from 400 to 500. For the convenience in the programming, the length of data is uniformly chosen as 400 points in our study.

In other words, there are 400 sets of real-time signals, each set consists of a signal recorded from accelerometer, denoted as $X_a(t)$, and a signal recorded from gyroscope, denoted as $X_g(t)$, which will be used in the calculation of ICC.

Next, the speed in stance phase is calculated according to duration from the beginning of early stance phase to the end of late stance phase. In our experiments, it was found that the fast speed defined in Section III-A-1 (i.e., the speed is 3 km/h or higher) corresponds to the duration of stance phase, which is 0.86 s or lower, the medium speed defined there corresponds to the duration of stance phase from 0.86 s to 0.92 s, and the slow speed is corresponding to the duration of stance phase, which is 0.92 s or higher. Therefore,the walking speed can be inferred from the duration time of stance phase. It has two functions. On one hand, it is inputted to the prosthesis controller to adjust the controller parameters for different speed. On the other hand, it is used to choose the terrain samples according to the corresponding speeds defined in Section A-1 Five terrain samples of the corresponding speed (e.g., fast speed or slow speed) are set as $Y_{ai}(t)$ and $Y_{gi}(t)$, which will also be used in the calculation of ICC. Finally, the ICC of real-time signals and 5 samples data with similar speed are calculated one by one as below:

$$C_{\mathrm{acc}}(i)=\frac{E(X_a(t)Y_{ai}(t))-E(X_a(t))E(Y_{ai}(t))}{\sqrt{E(X_a(t)^2)-E(X_a(t))^2}\sqrt{E(Y_{ai}(t)^2)-E(Y_{ai}(t))^2}} \tag{1}$$

$$C_{\mathrm{gyr}}(i)=\frac{E(X_g(t)Y_{gi}(t))-E(X_g(t))E(Y_{gi}(t))}{\sqrt{E(X_g(t)^2)-E(X_g(t))^2}\sqrt{E(Y_{gi}(t)^2)-E(Y_{gi}(t))^2}} \tag{2}$$

where $i = 1, \ldots, 5$.

In ideal conditions, the ICC coefficients of the corresponding terrain are the highest number in the same group. However, there are inevitable errors caused by interference, randomness in human motion, and the insufficient data. For example, there are five groups of the terrain test in our experiments, each including 100 steps. The data are sampled and processed via the ICC. The accurate ratio of recognition via accelerometer is 379 out of 500 while the accurate ratio of gyroscope is 353 out of 500, as shown in Table I and Table II. This test suggests that the ICC coefficients should be further treated in a more sophisticated manner.

TABLE I
ACCURACY RATE VIA ACCELEROMETER ICC

Terrain	SA	SD	UR	DR	LG	Accuracy
Stair ascent (SA)	83	1	10	2	4	83 %
Stair descent (SD)	1	80	3	11	5	80 %
Up ramp (UR)	14	2	69	5	10	69 %
Down ramp (DR)	2	16	2	70	10	70 %
Level ground (LG)	4	3	11	5	77	77 %
Total	-	-	-	-	-	75.8 %

TABLE II
ACCURACY RATE VIA GYROSCOPE ICC

Terrain	SA	SD	UR	DR	LG	Accuracy
Stair ascent (SA)	71	4	12	3	10	71 %
Stair descent (SD)	3	69	2	14	12	69 %
Up ramp (UR)	11	1	73	6	9	73 %
Down ramp (DR)	3	15	3	66	13	66 %
Level ground (LG)	4	5	8	9	74	74 %
Total	-	-	-	-	-	70.6 %

B. Sensor Fusion

Sensor fusion is the combination of data from separate sources, such that the resulted information is better than the one obtained by individual sensor.Sensor fusion has been widely used in prosthetic control field. For instance, [26] fused the implantable sensors and wearable inertial sensors to estimate the knee joint angle, via the technique of maximum entropy ordered weighted averaging (MEOWA). Reference [27] fused the data from surface EMG signals and gyroscope signals to estimate the intended knee joint angle, by using the Levenberg-Marquardt neural network. Among the available sensor fusion algorithms, Dempster-Shafer's (D-S) theory is the mature one with good feasibility and reliability [28]−[30].

To implement sensor fusion via D-S theory, one needs to define a hypothesis space $\Theta = \{SA, SD, UR, DR, LG, \emptyset\} := \{1, 2, 3, 4, 5, 0\}$, where SA = 1 stands for stair ascent, SD = 2 for stair descent, UR = 3 for up ramp, DR = 4 for down ramp, and LG = 5 for level ground, respectively. In this way, an identification framework for the terrain recognition is established, which includes five focal elements.

The mass function of basic probability assignment should satisfy the following conditions:

$$\sum_{i\in\Theta} m(i) = \sum_{i=0}^{5} m(i) = 1, \quad m(i) \geq 0 \tag{3}$$

where $m(i)$ is the probability of the event $i \in \Theta$. For instance, in Table III, $m_{\rm acc}(SD) = m_{\rm acc}(2) = 0.098$. Similarly, $C_{\rm gyr}(LG) = C_{\rm gyr}(5) = 0.811$.

Following the Dempster's combinational rules, we first build an evidence combination table, as shown in Table III. The effectiveness of the sensor fusion algorithm based on the D-S theory can be demonstrated by the following simple case. Take a set of sensor data of walking on the level ground (LG = 5) as an example, in which the ICC of gyroscope is $C_{\rm gyr}(5) = C_{\rm gyr}(LG) = 0.254$ that is smaller than $C_{\rm gyr}(1) = C_{\rm gyr}(SA) = 0.257$ (the SA terrain); the ICC of accelerator is $C_{\rm acc}(5) = C_{\rm acc}(LG) = 0.240$ that is smaller than $C_{\rm acc}(3) = C_{\rm acc}(UR) = 0.258$ (the UR terrain); and hence indicating inconsistence with the real LG terrain. However, with the aid of D-S theory, in particular, by computing the combined probability based on (5), we obtain $m_{\rm com}(5) = m_{\rm com}(LG) = 0.311$ which is strictly bigger than $m_{\rm com}(1) = m_{\rm com}(SA) = 0.261$ and $m_{\rm com}(3) = m_{\rm com}(UR) = 0.248$, and thus concluding that the real terrain is LG, not SA or UR. Therefore, the uncertainty and incorrectness in the original sensor data can be remedied by the sensor fusion method based on the D-S theory.

TABLE III
EVIDENCE COMBINATION TABLE

	$C_{\rm gyr}$	$m_{\rm gyr}(\cdot)$	$C_{\rm acc}$	$m_{\rm acc}(\cdot)$	$m_{\rm com}(\cdot)$
SA = 1	0.852	0.257	0.637	0.192	0.261
SD = 2	0.315	0.095	0.324	0.098	0.049
UR = 3	0.604	0.182	0.856	0.258	0.248
DR = 4	0.437	0.132	0.462	0.139	0.097
LG = 5	0.811	0.254	0.795	0.240	0.311
$\emptyset$ = 0	0.294	0.089	0.242	0.073	0.034

The ICC is calculated by (1) and (2). The $C(\emptyset)$ in Table III represents the inaccuracy rates obtained from lab experiments, as shown in Table I and Table II. Specifically, the inaccuracy rate of the gyroscope ICC from Table II is $1-70.6\,\%$, which forms $C_{\rm gyr}(\emptyset) = C_{\rm gyr}(0)$ = 0.294 in Table III. Likewise, the inaccuracy rate of the accelerometer ICC from Table I is equal to $1 - 75.8\,\%$, which leads to $C_{\rm acc}(\phi) = C_{\rm acc}(0) = 0.242$ in Table III.

On the other hand, the mass functions, $i = 0, \ldots, 5$, are calculated by

$$m_{\rm acc}(i) = \frac{C_{\rm acc}(i)}{\sum\limits_{n=0}^{5} C_{\rm acc}(n)}, \quad m_{\rm gyr}(i) = \frac{C_{\rm gyr}(i)}{\sum\limits_{n=0}^{5} C_{\rm gyr}(n)} \tag{4}$$

while the combined probability $m_{\rm com}(i)$ is computed by

$$\begin{aligned} m_{\rm com}(i) &= m_{\rm acc}(i) \oplus m_{\rm gyr}(i) \\ &= \frac{1}{K} m_{\rm acc}(i) \cdot m_{\rm gyr}(i), \quad i = 0, \ldots, 5 \end{aligned} \tag{5}$$

where K is the normalized constant defined as

$$K = 1 - \sum_{i=0}^{5} \sum_{j=0, j\neq i}^{5} m_{\rm acc}(i) \cdot m_{\rm gyr}(j). \tag{6}$$

The calculated values based on (1), (2), (4), and (5) are listed in Table III. Table IV collects the overall accuracy rates in 500 sets of fused sensor data. It indicates that the sensor fusion method based on the D-S theory increases the accuracy rate to 87.4 % from 75.8 % of accelerometer ICC (see Table I) and the 70.6 % of gyroscope ICC (see Table II), respectively.

TABLE IV
ACCURACY RATE VIA SENSOR FUSION

Terrain	SA	SD	UR	DR	LG	Accuracy
Stair ascent (SA)	94	1	4	0	3	94 %
Stair descent (SD)	1	90	1	6	2	90 %
Up ramp (UR)	10	2	81	3	4	81 %
Down ramp (DR)	2	11	2	79	6	79 %
Level ground (LG)	1	0	4	2	93	93 %
Total	-	-	-	-	-	87.4 %

C. Hidden Markov Model

Hidden Markov model describes a double stochastic process. In HMM, the state transition is related with the prior state.The HMM is widely used in human motion and posture recognition.HMM was used for classifying six classes of upper extremity limb movement in [31], and it was illustrated that HMM has a higher classification accuracy. Reference [32] proposed a HMM-based silhouette reconstruction strategy for gait recognition, while [33] used HMM to detect the phases of human images and extract the human gaits in a walking cycle against the noisy background images, by using strong prior knowledge.

For human walking, the gait transition from one terrain to another is a hidden process that cannot be directly observed by the controller of prosthesis limb. The terrain recognition can only be deduced from the outer sensors. This type of process can naturally be described by HMM. Because there is an obvious regularity in the terrains where human are, some prior knowledge can be used in intent recognition for lower-limb motion. For example, if the first step is stair ascent, the next step would be either level ground or stair ascent. It is almost impossible to be stair descent or ramp in normal human environment. Besides, the two ends of ramp are usually level ground, not stair. Conversely, the two ends of stairs are usually level ground, not ramp. These rules are drawn from the regularity of road or building construction. Therefore, it is expected that a pattern recognition method combined with the general regularity would have a higher accuracy rate of terrain identification. Since the upcoming step is always based on the last step, the walking process can be described as a typical hidden Markov model with strong prior knowledge.

In this work, HMM is used for terrain recognition through a state transition manner. To describe the HMM-based approach, we introduce a five-state HMM λ defined by

$$\lambda = (N, M, \pi, A, B) \tag{7}$$

where N is the hidden state containing five possible terrains, namely, stair ascent (SA), stair descent (SD), up ramp (UR), down ramp (DR), and level ground (LG). M is the fused information from sensor data. π is the initial state probability vector defined as

$$\begin{aligned} \pi &= [\pi_1, \pi_2, \pi_3, \pi_4, \pi_5] \\ &= [0.2, 0.2, 0.2, 0.2, 0.2] \end{aligned} \tag{8}$$

where π_i is the initial probability of the ith terrain, set equally as 0.2. Note that according to Table III, each ith terrain corresponds to a unique walking pattern, for instance, $3 = UR = up\,ramp$.

Now, introduce a 5×5-dimensional matrix A which represents the state transition probability matrix. Clearly, the element $a_{i,j}$ in A is the probability of transition from last terrain state i to the upcoming state j. That is,

$$a_{i,j} = P(j|i), \quad 1 \le i; \quad j \le 5. \tag{9}$$

The state transition probability matrix in ideal condition, i.e., a normal environment, is given by

$$A = \begin{bmatrix} 0.5 & 0 & 0 & 0 & 0.5 \\ 0 & 0.5 & 0 & 0 & 0.5 \\ 0 & 0 & 0.5 & 0 & 0.5 \\ 0 & 0 & 0 & 0.5 & 0.5 \\ 0.2 & 0.2 & 0.2 & 0.2 & 0.2 \end{bmatrix}. \tag{10}$$

To see why it is so, let us take the third row as an example. If the prior motion is up ramp, the possibility of upcoming step for up ramp or level ground is 50 %. Consequently, $a_{3,3}$ and $a_{3,5}$ are both 0.5, while $a_{3,1} = a_{3,2} = a_{3,4} = 0$.

Finally, we introduce the state observation probability matrix B denoted as

$$B = [b_{i,j(O_t)}]_{1 \le i,j \le 5} = \begin{bmatrix} 0.94 & 0.01 & 0.04 & 0.00 & 0.01 \\ 0.01 & 0.90 & 0.01 & 0.06 & 0.02 \\ 0.10 & 0.02 & 0.81 & 0.03 & 0.04 \\ 0.02 & 0.11 & 0.02 & 0.79 & 0.06 \\ 0.01 & 0.00 & 0.04 & 0.02 & 0.93 \end{bmatrix} \tag{11}$$

which is obtained straightforwardly from Table IV, by simply dividing each element by 100 in Table IV.

Note that $b_{i,j(O_t)}$ in (11) is the observation probability of the state on the ith row and the $j(O_t)$th column of the matrix B, e.g., for $i = 4$ and $j(O_t) = 2$, $b_{4,2} = 0.06$. However, it should be noted that the determination of the column of B, namely, the number j depends on the so-called observation convector as shown in (12).

$$O_t = [o_1(t), o_2(t), o_3(t), o_4(t), o_5(t)] \in \mathbb{R}^{1\times 5} \tag{12}$$

where $t = 1, 2, 3, \ldots,$ are the step numbers, $o_l(t), l = 1, \ldots, 5$, are either equal to 0 or 1, and there is only one $o_l(t)$ whose value is 1, which is determined according to the highest value in the sensor fusion result. For example, if $o_3(t) = 1$ then $O_t = [0, 0, 1, 0, 0]$. Consequently,

$$j(O_t) = 3.$$

In other words, the one with $o_l(t) = 1$ reflects exactly the lth column of the matrix B. This selection rule is crucial for the recurring process of HMM below.

The element of O_t can be determined in the following manner. Using the data $m_{\mathrm{com}}(i)$ from Table III, one can compute the quantity

$$\max_{i=1,\ldots,5} m_{\mathrm{com}}(i).$$

Based on the quantity thus obtained, we can then determine exactly which $o_l(t)$ is equal to one. For instance, it is clear from Table III that at the step t,

$$\max_{i=1,\ldots,5} m_{\mathrm{com}}(i) = 0.311.$$

Hence, $o_5(t) = 1$ and thus $o_l(t) = 0$, for $l = 1, 2, 3, 4$. That is, at the step t,

$$O_t = [0, 0, 0, 0, 1].$$

With the help of the observation vector O_t and the prior state probabilities, the HMM can determine which state has the highest probability for the current state. The intended limb motion associated with the state of the highest probability is the classification decision for the current time index t.

The recurring process of HMM can be described by the following equations.

Initial step (t = 1):

$$\delta_i(t = 1) = \pi_i b_{i,5}, \ 1 \le i \le 5. \tag{13}$$

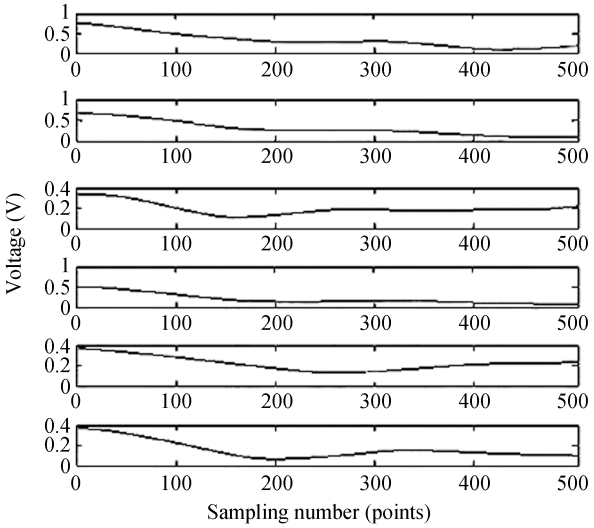

(a) Signals of accelerometer

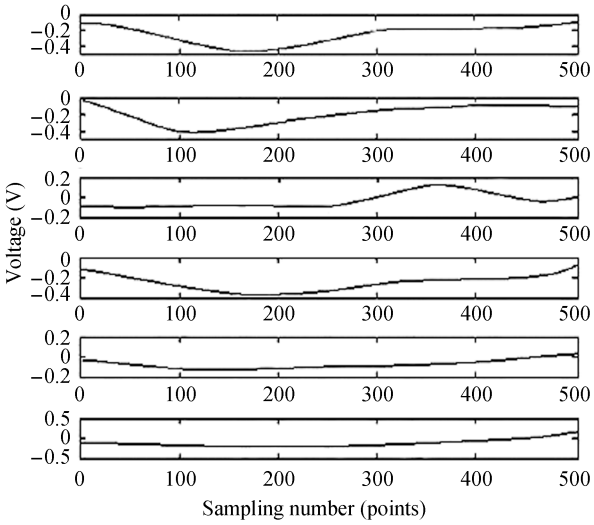

(b) Signals of gyroscope

Fig. 6. Intraclass correlation coefficient of real time signal and standard samples.

Inductive step ($t = 2, 3, \ldots, 500$):

$$\delta_i(t+1) = b_{i,j(O_{t+1})} \max_{k=1,\ldots,5} (\delta_k(t) a_{k,i}) \tag{14}$$

$$\phi_{t+1} = \arg \max_{i=1,\ldots,5} (\delta_i(t+1)) \tag{15}$$

where δ_i denotes the probability of the ith terrain, and ϕ denotes the current terrain. That is, ϕ_{t+1} is equal to one of the numbers 1, 2, 3, 4, 5, or is one of the terrains of SA, SD, UR, DR and LG. ϕ_{t+1} is then inputted to the prosthesis controller to adjust the controller parameters for different terrains in the upcoming swing phase.

As one can see in (14), the current state of HMM depends on the prior terrain state. In our experiments, the prior terrain state is retrospected to update the predicted state before starting a new cycle of prediction. This is important in improving the accuracy of the terrain recognition, simply because the terrain retrospect is based on the data of both stance phase and swing phase, while the terrain prediction is only based on the data of stance phase. As a result, the accuracy of retrospected result is always higher than that of predicted, as shown in Table V. The procedure of the prior terrain state updating is described as follows. Firstly, retrospect the prior terrain state via the method of ICC and sensor fusion, in which the data of stance phase and swing phase are used. Next, use the retrospected state to replace the predicted $\delta_k(t)$ in (14). Finally, the recursion of (14) is carried out step by step. Our experiments have demonstrated that the corrected prior state significantly improves the accuracy of the terrain recognition in the upcoming terrain recognition cycle.

TABLE V
TERRAIN RETROSPECTING

Terrain	SA	SD	UR	DR	LG	Accuracy
Stair ascent (SA)	99	0	1	0	0	99 %
Stair descent (SD)	0	99	0	1	0	99 %
Up ramp (UR)	1	0	99	0	0	99 %
Down ramp (DR)	0	1	0	97	2	97 %
Level ground (LG)	0	0	1	1	98	98 %
Total	-	-	-	-	-	98.4 %

IV. RESULTS AND DISCUSSION

Three healthy persons and two amputees participated in the experiment. In Fig. 7, a group of signals of healthy person and amputee are contrasted. Although the amplitudes are different, which are caused by the amputees' motion abilities, the signal trends are basically same. Therefore, the method in this paper works for both amputee and healthy person.

As some incorrect recognition of terrain is removed by HMM, the final accuracy rate rises from 87.4 % to 95.8 %, as shown in the Table VI. And the accuracy rates of each terrain are shown in Fig. 8.

As the transition probabilities between level ground to other terrains are all equal to 0.2, so the terrain recognition based on HMM for level ground seems not as effective as the other terrains.As far as the defect of HMM in level ground is concerned, [33] proposed a wearable laser distance sensor to detect the terrain change in front of the prosthesis user. It might be an effective way, and this method would be integrated in the future. The results of this study suggest that the proposed approach is practically feasible and effective for the design of general mechanical sensor-based above-knee prosthesis. However, continuing efforts will be required to include other activities of daily life such as standing up, sitting, bicycle riding, etc. These issues will be investigated in our future work.

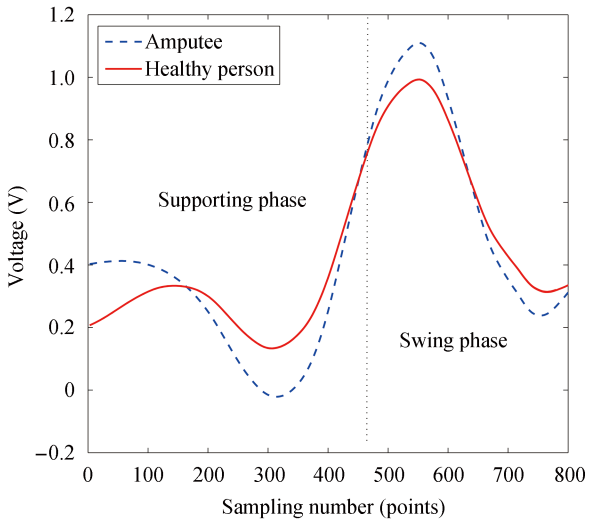

(a) Signal contrast of acceleration

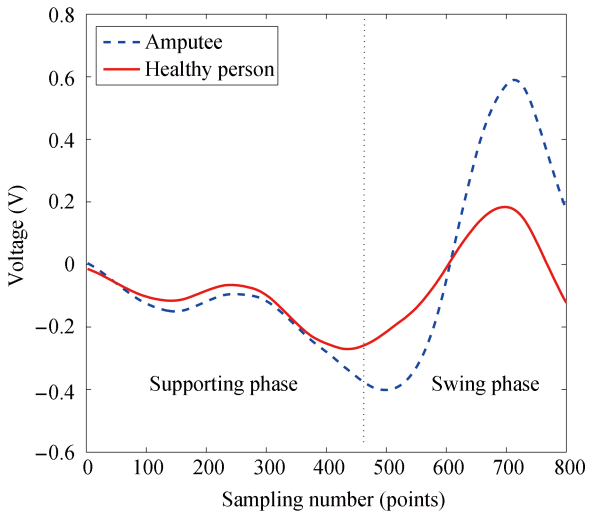

(b) Signal contrast of gyroscope

Fig. 7. Signal contrast.

TABLE VI
ACCURACY RATE VIA HMM

Terrain	SA	SD	UR	DR	LG	Accuracy
Stair ascent (SA)	99	0	0	0	1	99 %
Stair descent (SD)	0	98	0	0	2	98 %
Up ramp (UR)	1	0	95	0	4	95 %
Down ramp (DR)	0	0	0	94	6	94 %
Level ground (LG)	1	0	4	2	93	93 %
Total	-	-	-	-	-	95.8 %

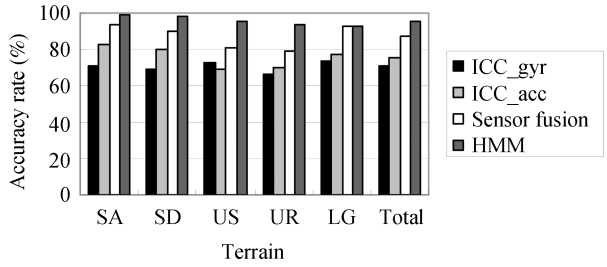

Fig. 8. Increasing correct rate of terrain recognition.

It should be pointed out that the method proposed in this paper has some limitations. For instance, when the amputee walks in complex terrains such as the lawn or uneven road, it appears that our method cannot work as effectively as in the normal terrains. To address such an issue, the EMG-based prosthesis may be an alternative if bottlenecks of EMG signals processing such as interference, electrode shifting, sweat and so on can be solved. This is because the EMG-based prosthesis is controlled directly by the amputee's residual muscles, and therefore reflecting the amputee's movement intention more accurately [34].

V. Conclusion

This paper has proposed an intent pattern recognition approach based on mechanical sensors for above-knee prosthesis. By comparison, the proposed method has certain advantages over the EMG-based prosthesis, such as convenient in use, lower cost and better reliability. In addition, because of using the data of stance phase, the method proposed in this paper can predict the terrain patterns in the upcoming swing with the accuracy rate of 95.8 %. It has, in lab experiments, substantially improved the control performance of powered above-knee prothesis.

Acknowledgment

The authors would like to thank Professor Xitai Wang at the National Research Center for Rehabilitation Technical Aids of China, Dr. Lingling Chen at the Engineering Research Center of Intelligent Rehabilitation, Ministry of Education of China, for their assistance with the experiments reported in this paper. We would also like to thank Dr. Haiyong Chen, Dr. Guansheng Xing, and Dr. Dedong Yang at Hebei University of Technology for their helpful discussions.

References

[1] H. Huang, T. A. Kuiken, and R. D. Lipschutz, "A strategy for identifying locomotion modes using surface electromyography," *IEEE Trans. Biomed. Eng.*, vol. 56, no. 1, pp. 65−73, Jan. 2009.

[2] H. A. Varol, F. Sup, and M. Goldfarb, "Multiclass real-time intent recognition of a powered lower limb prosthesis," *IEEE Trans. Biomed. Eng.*, vol. 57, no. 3, pp. 542−551, Mar. 2010.

[3] P. Yang, Z. J. Liu, Y. L. Geng, and L. N. Zhao, "Research advance on key technology of intelligent lower limb prosthesis," *J. Hebei. Univ. Technol.*, vol. 42, no. 1, pp. 76−80, Feb. 2013.

[4] J. D. Miller, M. S. Beazer, and M. E. Hahn, "Myoelectric walking mode classification for transtibial amputees," *IEEE Trans. Biomed. Eng.*, vol. 60, no. 10, pp. 2745−2750, Oct. 2013.

[5] X. R. Zhang, Y. H. Liu, F. Zhang, J. Ren, Y. L. Sun, Q. Yang, and H. Huang, "On design and implementation of neural-machine interface for artificial legs," *IEEE Trans. Industr. Inform.*, vol. 8, no. 2, pp. 418−429, May 2012.

[6] A. Presacco, L. W. Forrester, and J. L. Contreras-Vidal, "Decoding intra-limb and inter-limb kinematics during treadmill walking from scalp electroencephalographic (EEG) signals," *IEEE Trans. Neural Syst. Rehabil. Eng.*, vol. 20, no. 2, pp. 212−219, Mar. 2012.

[7] H. Huang, F. Zhang, L. J. Hargrove, Z. Dou, D. R. Rogers, and K. B. Englehart, "Continuous locomotion-mode identification for prosthetic legs based on neuromuscular-mechanical fusion," *IEEE Trans. Biomed. Eng.*, vol. 58, no. 10, pp. 2867−2875, Oct. 2011.

[8] L. Du, F. Zhang, M. Liu, and H. Huang, "Toward design of an environment-aware adaptive locomotion-mode-recognition system," *IEEE Trans. Biomed. Eng.*, vol. 59, no. 10, pp. 2716−2725, Oct. 2012.

[9] E. H. Zheng, L. Wang, K. L. Wei, and Q. N. Wang, "A noncontact capacitive sensing system for recognizing locomotion modes of transtibial amputees," *IEEE Trans. Biomed. Eng.*, vol. 61, no. 12, pp. 2911−2920, Dec. 2014.

[10] A. J. Young, L. J. Hargrove, and T. A. Kuiken, "Improving myoelectric pattern recognition robustness to electrode shift by changing interelectrode distance and electrode configuration," *IEEE Trans. Biomed. Eng.*, vol. 59, no. 3, pp. 645−652, Mar. 2012.

[11] Q. C. Ding, A. B. Xiong, X. G. Zhao, and J. D. Han, "A review on researches and applications of sEMG-based motion intent recognition methods," *Acta Automat. Sin.*, vol. 42, no. 1, pp. 13−25, Jan. 2016.

[12] L. Shen and H. L. Yu, "Development course of prosthetics at home and abroad," *Chin. J. Tiss. Eng. Res.*, vol. 16, no. 13, pp. 2451−2454. Mar. 2012.

[13] Y. L. Geng, Y. Pang, Z. J. Liu, and X. R. Wang, "Walking speed recognition system for transfemoral amputee based on accelerometer and gyroscopes," in *System Simulation and Scientific Computing*, Shanghai, China, 2012, pp. 383−389.

[14] X. R. Zhang, D. Wang, Q. Yang, and H. Huang, "An automatic and user-driven training method for locomotion mode recognition for artificial leg control," in *Proc. of Annu. Int. Conf. IEEE Engineering in Medicine and Biology Society*. San Diego, CA, USA, 2012.

[15] Y. Y. Gao, Q. S. She, M. Meng, and Z. Z. Luo, "Recognition method based on multi-information fusion for gait patterns of above-knee prosthesis," *Chin. J. Sci. Instrum.*, vol. 31, no. 12, pp. 2682−2688, Dec. 2010.

[16] F. Sup, H. A. Varol, and M. Goldfarb, "Upslope walking with a Powered knee and ankle prosthesis: initial results with an amputee subject," *IEEE Trans. Neural Syst. Rehabil. Eng.*, vol. 19, no. 1, pp. 71−78, Feb. 2011.

[17] X. G. Wang, Q. N. Wang, E. H. Zheng, K. L. Wei, and L. Wang, "A wearable plantar pressure measurement system: Design specifications and first experiments with an amputee," in *in Proc. the 12th Int. Conf. Intelligent Autonomous Systems*, Jeju Island, Korea, 2012, pp. 273−281.

[18] B. J. Chen, E. H. Zheng, X. D. Fan, T. Liang, Q. N. Wang, K. L. Wei, and L. Wang, "Locomotion mode classification using a wearable capacitive sensing system," *IEEE Trans. Neural Syst. Rehabil. Eng.*, vol. 21, no. 5, pp. 744−755, Sep. 2013.

[19] K. B. Yuan, Q. N. Wang, and L. Wang, "Fuzzy-logic-based terrain identification with multisensor fusion for transtibial amputees," *IEEE/ASME Trans. Mechatron.*, vol. 20, no. 2, pp. 618−630, Apr. 2015

[20] A. J. Young, A. M. Simon, and L. J. Hargrove, "A training method for locomotion mode prediction using powered lower limb prostheses," *IEEE Trans. Neural Syst. Rehabil. Eng.*, vol. 22, no. 3, pp. 671−677, May 2014.

[21] Y. D. Li and E. T. Hsiao-Wecksler, "Gait mode recognition and control for a portable-powered ankle-foot orthosis," *in Proc. 2013 IEEE Int. Conf. Rehabilitation Robotics*, Seattle, WA, USA, 2013, pp. 1−8.

[22] G. M. Leigh, "Fast FIR algorithms for the continuous wavelet transform

from constrained least squares," *IEEE Trans. Signal Process.*, vol. 61, no. 1, pp. 28−37, Jan. 2013.

[23] A. G. Polimeridis, and J. R. Mosig, "Evaluation of weakly singular integrals via generalized cartesian product rules based on the double exponential formula," *IEEE Trans. Antennas Propag.*, vol. 58, no. 6, pp. 1980−1988, Jun. 2010.

[24] A. S. Anna, A. Salarian, and N. Wickstrom, "A new measure of movement symmetry in early parkinsons disease patients using symbolic processing of inertial sensor data," *IEEE Trans Biomed. Eng.*, vol. 58, no. 7, pp. 2127−2135, Jul. 2011.

[25] M. L. Audu, C. S. To, R. Kobetic, and R. J. Triolo, "Gait evaluation of a novel hip constraint orthosis with implication for walking in paraplegia," *IEEE Trans. Neural Syst. Rehabil. Eng.*, vol. 18, no. 6, pp. 610−618, Dec. 2010.

[26] A. Arami, A. Barré, R. Berthelin, and K. Aminian, "Estimation of prosthetic knee angles via data fusion of implantable and wearable sensors," in *Proc. of IEEE Int. Conf. Body Sensor Networks*, Cambridge, MA, USA, 2013, pp. 1−6.

[27] A. L. Delis, J. L. A. de Carvalho, G. A. Borges, S. de Siqueira Rodrigues, I. dos Santos, and A. F. da Rocha, "Fusion of electromyographic signals with proprioceptive sensor data in myoelectric pattern recognition for control of active transfemoral leg prostheses," in *Proc. of Annu. Int. Conf. the Engineering in Medicine and Biology Society*, Minneapolis, MN, USA, 2009, pp. 4755−4758.

[28] R. R. Murphy, "Dempster-Shafer theory for sensor fusion in autonomous mobile robots," *IEEE Trans. Robot. and Automat.*, vol. 14, no. 2, pp. 197−206, Apr. 1998.

[29] S. Foucher, M. Germain, J. M. Boucher, and G. B. Benie, "Multisource classification using ICM and Dempster-Shafer theory," *IEEE Trans. Instrum. Meas.*, vol. 51, no. 2, pp. 277−281, Apr. 2002.

[30] F. Delmotte and P. Smets, "Target identification based on the transferable belief model interpretation of Dempster-Shafer model," *IEEE Trans. Syst. Man Cybern. A Syst. Hum*, vol. 34, no. 4, pp. 457−471, Jul. 2004.

[31] A. D. C. Chan and K. B. Englehart, "Continuous myoelectric control for powered prostheses using hidden Markov models," *IEEE Trans. Biomed. Eng.*, vol. 52, no. 1, pp. 121−124, Jan. 2005.

[32] Z. Y. Liu and S. Sarkar, "Effect of silhouette quality on hard problems in gait recognition," *IEEE Trans. Syst. Man Cybern. B*, vol. 35, no. 2, pp. 170−183, Apr. 2005.

[33] Z. H. Zhou, A. Prugel-Bennett, and R. I. Damper, "A Bayesian framework for extracting human gait using strong prior knowledge," *IEEE Trans Pattern Anal. Mech. Intell.*, vol. 28, no. 11, pp. 1738−1752, Nov. 2006.

[34] L. N. Tong, Z. G. Hou, L. Peng, W. Q. Wang, Y. X. Chen, and M. Tan, "Multi-channel sEMG time series analysis based human motion recognition method," *Acta Automat. Sin.*, vol. 40, no. 5, pp. 810−821, May 2014.

Zuojun Liu received the B.S. degree in the automation from Hebei University of Technology, Tianjin, China, in 1994, and M.S degree in the control theory and control engineering from Hebei University of Technology, Tianjin, China, in 2000, and B.A of English from Nankai University, Tianjin, China, in 2000, and Ph.D degree in the control theory and control engineering from Nankai University, Tianjin, China, in 2004. He completed his visiting scholar research at Nanyang Technological University, Singapore, in 2004 and CASE Western Reserve University, U.S in 2013, respectively. He is currently a Professor at the School of Control Science and Engineering, Hebei University of Technology. He is also with the Engineering Research Center of Intelligent Rehabilitation, Ministry of Education of China. His research interests include rehabilitation engineering, robotics, learning control, intelligent building and smart grid.

Wei Lin received the D.Sc. and M.S. degrees in systems science and mathematics from Washington University, St. Louis, MO, USA, in 1993 and 1991, M.S. degree from Huazhong University of Science and Technology in 1986 and B.S. from Dalian University of Science and Technology in 1983, both in electrical engineering. During 1986−1989, he was a Lecturer in the Department of Mathematics, Fudan University, Shanghai, China. From 1994 to 1995, he was a Post-doctor and a Visiting Assistant Professor in Washington University. Since Spring of 1996, he has been a Professor in the Department of Electrical Engineering and Computer Science, Case Western Reserve University, Cleveland, OH, USA. His current research interests include nonlinear control, time-delay systems, homogeneous systems theory, estimation and adaptive control, renewable energy, power systems and smart grids. In these areas, he has published more than 200 papers in peer-refereed journals and conferences.

Dr. Lin was a recipient of the NSF CAREER Award, the Warren E. Rupp Endowed Professorship, and the Robert Herbold Faculty Fellow Award. He served as an Associate Editor of the *IEEE Trans. on Automa. Contr.* (1999-2002), a Guest Editor of the Special Issue on New Directions in Nonlinear Control in the *IEEE Trans. on Automatic Control* (2003), an Associate Editor of *Automatica* (2003-2005), an Associate Editor of *Journal of Control Theory and Applications* (2005-2008), a Subject Editor (2005-2010) and Associate Editor (2011-present) of the *Int. J. of Robust and Nonlinear Control*.

Yanli Geng received the B.S. degree in the control technology and instruments from Agricultural University of Hebei, Hebei, China, in 2006, and M.S degree in the control theory and control engineering from Hebei University of Technology, Tianjin, China, in 2009, and Ph.D degree in the control theory and control engineering from Hebei University of Technology, Tianjin, China, in 2012. She is currently a Lecturer at the School of Control Science and Engineering, Hebei University of Technology. She is also with the Engineering Research Center of Intelligent Rehabilitation, Ministry of Education of China. Her research interests include rehabilitation engineering, intelligent control and robotics.

Peng Yang received the B.S. degree in the automation from Hebei University of Technology, Tianjin, China, in 1982, and M.S degree in the control theory and control engineering from Haerbing Institute of Technology, Heilongjiang, China, in 1986, and Ph.D degree in the electrical engineering from Hebei University of Technology, Tianjin, China, in 1998. He completed his visiting scholar research at Technical University of Munich, Germany, in 2005. He is currently a Professor at the School of Control Science and Engineering, Hebei University of Technology. He is also with the Engineering Research Center of Intelligent Rehabilitation, Ministry of Education of China. His research interests include rehabilitation engineering, intelligent control and robotics.